Molecular Biology of the Cell
Vol. 18, 66–75, January 2007

Fibronectin Matrix Assembly Requires Distinct Contributions from Rho Kinases I and -II[D]

Atsuko Yoneda, Dmitriy Ushakov, Hinke A.B. Multhaupt, and John R. Couchman

Division of Biomedical Sciences, Imperial College London, London SW7 2AZ, United Kingdom

Submitted August 7, 2006; Revised October 2, 2006; Accepted October 13, 2006
Monitoring Editor: Richard Assoian

Extracellular matrix is integral to tissue architecture and regulates many aspects of cell behavior. Fibronectin matrix assembly involves the actin cytoskeleton and the small GTPase RhoA, but downstream signaling is not understood. Here, down-regulation of either rho kinase isoform (ROCK I or -II) by small interfering RNA treatment blocked fibronectin matrix assembly, although the phenotypes were distinct and despite persistence of the alternate kinase. Remnant fibronectin on ROCK-deficient fibroblasts was mostly punctate and more deoxycholate soluble compared with controls. Fibronectin matrix assembly defects in ROCK-deficient cells did not result from decreased synthesis/secretion, altered fibronectin mRNA splicing, metalloproteinase activity, or $\alpha 5\beta 1$ integrin dysfunction. Rescue could be effected by ROCK protein restoration or phosphomimetic myosin light chain expression. However, the effect of ROCK I deficiency on fibronectin matrix assembly was secondary to altered cell surface morphology, rich in filopodia, resulting from high GTP–Cdc42 levels. Total internal reflection microscopy revealed that a submembranous pool of myosin light chain in control cells was missing in ROCK II-deficient cells and replaced by stress fibers. Together, two rho kinases contribute to fibronectin matrix assembly in a different manner and cortical myosin II-driven contractility, but not stress fibers, may be critical in this activity.

INTRODUCTION

Cells such as fibroblasts are responsible for synthesis, assembly, and turnover of extracellular matrix. The assembly of fibronectin (FN)-rich matrices at the cell surface is integral to this process because FN can interact with cell surface receptors such as integrins and proteoglycans, and with extracellular matrix collagen, fibrin, and FN itself. The process of FN matrix assembly is known to depend on several factors (for review, see Mao and Schwarzbauer, 2005). The binding of secreted FN dimers to integrin is an early step, accompanied by an unfolding mechanism, because soluble FN is compact and not competent in polymerization. For many cells, the $\alpha 5\beta 1$ integrin fills this role, and microscopy indicates that it can be translocated from focal adhesions into fibrillar adhesions, rich in FN and tensin, but poor in the focal adhesion protein paxillin (Katz *et al*., 2000). Conformational changes in FN may be assisted by tension that unfolds molecules (Zhong *et al*., 1998; Baneyx *et al*., 2002), allowing self-association through several sites, but the 70-kDa amino-terminal fragment is particularly important. Binding of other cell surface molecules such as glycosaminoglycans may additionally potentiate FN matrix formation (Klass *et al*., 2000). Also known to be essential is an intact actin cytoskeleton, and FN matrix assembly is promoted by GTP-RhoA (Zhong *et al*., 1998) that itself promotes actin microfilament bundle and focal adhesion formation (Etienne-Manneville and Hall, 2002; Burridge and Wennerberg, 2004). Lysophosphatidic acid, present in serum, acting through cell surface receptors can signal increases in GTP-RhoA and enhances FN matrix deposition (Zhang *et al*., 1997).

The processes downstream of RhoA in terms of FN matrix assembly are not well understood, but they could involve rho kinases (ROCKs) and their regulation of myosin II, also leading to microfilament bundle formation. However, there are several downstream effectors of RhoA besides the rho kinases (Bishop and Hall, 2000). Moreover, our recent study indicates that the two widely distributed homologous rho kinases may not be functionally equivalent (Yoneda *et al*., 2005). The use of small interfering RNA (siRNA) and other techniques indicates that in fibroblasts, ROCK I is of much greater significance for stress fiber and focal adhesion assembly, whereas ROCK II has a role in FN matrix endocytosis or macropinocytosis. This is despite similar substrates for the two ROCKs, myosin light chain (MLC) and the myosin-binding subunit of myosin phosphatase.

In this study, we examine the hypothesis that although the two ROCKs are both downstream of GTP-RhoA, they may have distinct roles with respect to the actin cytoskeleton requirements for FN matrix assembly.

This article was published online ahead of print in *MBC in Press* (http://www.molbiolcell.org/cgi/doi/10.1091/mbc.E06–08–0684) on October 25, 2006.

[D] The online version of this article contains supplemental material at *MBC Online* (http://www.molbiolcell.org).

Address correspondence to: John R. Couchman (j.couchman@imperial.ac.uk).

Abbreviations used: DOC, deoxycholate; ERM, ezrin/radixin/moesin; FN, fibronectin; MLC, myosin light chain; REF, rat embryo fibroblasts; TIRF, total internal reflection microscopy.

MATERIALS AND METHODS

Antibodies

Rabbit polyclonal anti-FN (R2/7) was made against bovine plasma FN (McCarthy *et al*., 1993). Mouse monoclonal anti-FN (L8) was a generous gift from Dr. M. A. Chernousov (Geisinger Clinic, Danville, PA). Monoclonal anti-myc (9E10) was purchased from Sigma-Aldrich (St. Louis, MO). Polyclonal antibodies against actin were from Santa Cruz Biotechnology (Santa Cruz, CA). A polyclonal antibody against phospho-Ezrin(Thr567)/Radixin (Thr564)/Moesin(Thr558) was from Cell Signaling Technology (Beverly, MA). Monoclonal anti-Tensin and anti-Cdc42 were from BD Transduction Laboratories (Lexington, KY). Rabbit polyclonal $\alpha 5$ integrin and $\beta 1$ integrin antibod-

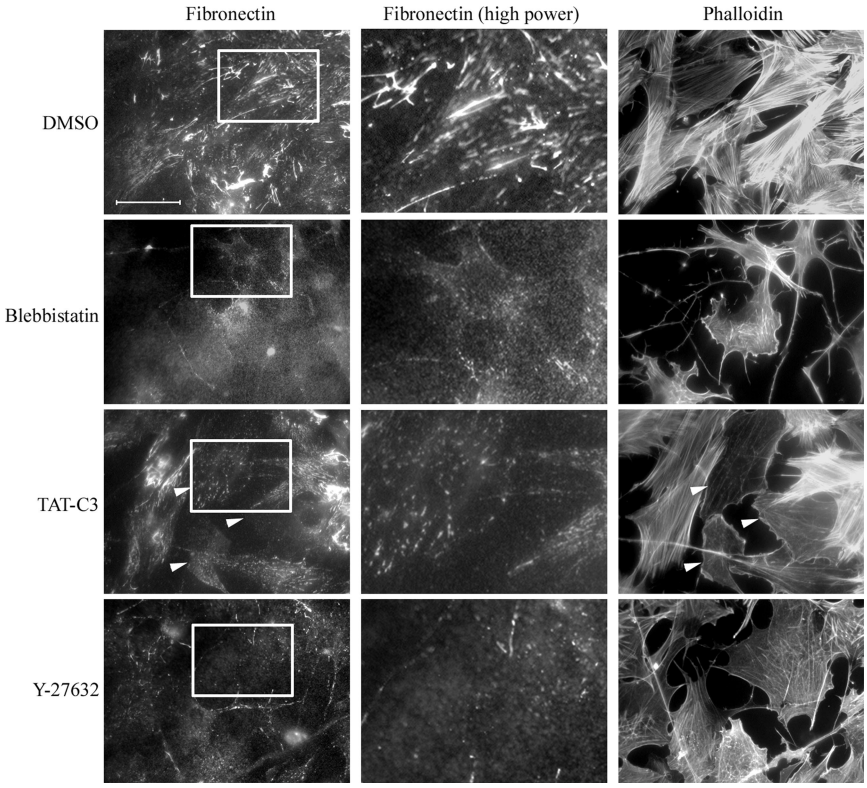

Figure 1. Rho/rho kinase pathway is required for FN matrix assembly. REFs were plated in the presence of serum for 30–40 min and 15 μM blebbistatin, 45 μg/ml TAT-C3, 30 μM Y-27632, or DMSO was added to the medium. Cells were incubated overnight, fixed, and stained for FN and F-actin. Arrowheads denote cells that incorporated TAT-C3. Bar, 50 μm. High-power micrographs (2.7× magnification) of FN staining in the center show corresponding areas boxed in the left micrographs.

ies were from Chemicon International (Temecula, CA). Peroxidase-conjugated rabbit-anti-goat IgG and swine anti-rabbit IgG were from Dako UK (Ely, Cambridgeshire, United Kingdom). Alexa Fluor 488/568/647-conjugated goat-anti-mouse or -rabbit were from Invitrogen (Paisley, United Kingdom).

Plasmids

Double point mutations in rat MLC (T18D, S19D) were created by polymerase chain reaction (PCR) of the whole pGEX-2T-MLCwt plasmid by using primers 146, 5′-GACAACGTGTTCGCCATGTTTGACCAG, and 145, 5′-ATCTGCGCGCTGAGGGCGCTTTTTGG, with KOD hot start polymerase (Novagen, Madison, WI). After digestion with DpnI (Invitrogen), the PCR product was phosphorylated by T4 polynucleotide kinase and self-ligated by T4 DNA ligase (Invitrogen). After sequence verification, PCR was carried out using primers 144, 5′-GCGAATTCCGCCACCATGTCGAGCAAAAAAGCAAAG and 147, 5′-GCGGATCCGCGTCATCTTTGTCTTTCGCTCCGTG, with KOD polymerase. The PCR product was digested with EcoRI and BamHI, ligated into pEGFP-N1 (Clontech, Mountain View, CA) and confirmed by DNA sequencing (MLC-DD-pEGFP-N1). Wild-type MLC-pEGFP-N1 was constructed by PCR by using pGEX-2T-MLCwt as template and primers 144/147 as described for MLC-DD-pEGFP-N1. GST-PAK CRIB construct was a kind gift from A. Hall (University College London, United Kingdom), pCAG-myc-p160ROCK(WT) was from S. Narumiya (Kyoto University, Kyoto, Japan), pEF-BOS-myc-Rho kinase (p164) and pGEX-2T-MLCwt were from K. Kaibuchi (Nagoya University, Nagoya, Japan), TAT-C3 (Sebbagh *et al*., 2001) was from J. Bertoglio (Institut National de la Santé et de la Recherche Médicale, Chatenay-Malabry, France), and pRK5-myc-N17-Cdc42 was from V. Braga (Imperial College London, United Kingdom). pRK5-myc-wild type Cdc42 were made by point mutation of N17-Cdc42 to T17.

FN Matrix Analysis and Immunofluorescence Microscopy

For double staining of extracellular FN and tensin or F-actin, rat embryo fibroblasts (REFs) were fixed with 4% paraformaldehyde (PFA) in phosphate-buffered saline (PBS) for 20 min, blocked with 5% bovine serum albumin (BSA) in PBS, and incubated with anti-FN antibody at 1:1000 dilution. Cells were then permeabilized with 0.1% Triton X-100 in PBS for 10 min. After blocking with 5% BSA in PBS, cells were incubated with tensin antibody at 1:100 dilution followed by incubation with appropriate fluorochrome-conjugated secondary antibodies or phalloidin (Alexa Fluor 488/568/647; Invitrogen). To assess FN matrix assembly phenotype, observer-based scoring was performed. FN matrix-positive cells were defined as possessing multiple fibrils, where at least two, or more, intersected. At least 50 cells were counted per experimental variable, and percentages of cells with fibrillar FN were compared from at least three independent experiments. For α5 and β1 integrin staining, cells were fixed with methanol at −20°C for 5 min. Controls for nonspecific cross-reaction of secondary antibodies were included and gave no staining above background. Samples were analyzed on an Olympus Provis AX module fluorescence microscope (UPlanApo 60× numerical aperture [NA] 1.4 objective; images were collected by a SPOT Insight Mono digital camera) or on a DM IRBE microscope (Leica Microsystems, Deerfield, IL) containing a krypton-argon laser and TCS NT software (Fluorotar 100× NA 1.4 objective) or on a Nikon ECLIPSE C1si system (Plan Apo VC 60× NA 1.40 objective; images were collected by a D-ECLIPSE camera), and images were processed using Adobe Photoshop 7.0 (Adobe Systems, Mountain View, CA). To examine the effects of actin cytoskeleton disruption, REFs in α-minimal essential medium with 5% fetal calf serum (FCS) were replated onto coverslips for 30–40 min and TAT-C3 (45 μg/ml), (−)-blebbistatin (15 μM; Merck Biosciences, Darmstadt, Germany), Y-27632 (30 μM; Merck Biosciences), or dimethyl sulfoxide (DMSO) were added to the medium. Cells were incubated overnight and processed for immunofluorescence microscopy.

Silencing of Rho Kinases

Target sequences for ROCK I and ROCK II were described previously (Yoneda *et al*., 2005). Transfection of 200 nM siRNA was carried out using Oligofectamine reagent (Invitrogen). Effective gene silencing was observed at the 50 nM level. At 48 h after transfection, cells were analyzed. Cotransfection of Cy3-labeled siRNA duplexes with plasmids was carried out in control experiments. To further inhibit rho kinase activity, 30 μM Y-27632 treatment was carried out for 4.5 h after 2 d of siRNA transfection. For metalloproteinase inhibition, 10 μM GM6001 (Merck Biosciences) or DMSO alone as control was added to the medium as REFs were transfected with siRNA, and growth medium containing fresh GM6001 or vehicle was exchanged after 1 d.

Total Internal Reflection Fluorescence (TIRF) Microscopy

REFs were cotransfected with siRNA duplex and MLCwt-pEGFP-N1 by using Oligofectamine. After 2 d, living cells were analyzed. Fluorescence images were obtained on an Axiovert 200 inverted microscope (Carl Zeiss, Jena, Germany) modified for objective-type TIRF (Till Photonics, Gräfelfing, Germany). An argon laser was used to excite green fluorescent protein (GFP) fluorescence at 488 nm through a 100 × 1.45 NA Planofluar objective (Carl Zeiss). During observation, the cells were kept at 37°C on MS2000 stage (Applied Scientific Instruments, Eugene, OR) equipped with a Focht chamber system (FCS2; Bioptechs, Butler, PA). Images were recorded with a PCO SensiCam charge-coupled device camera and analyzed using ImageJ software (http://rsb.info.nih.gov/ij/).

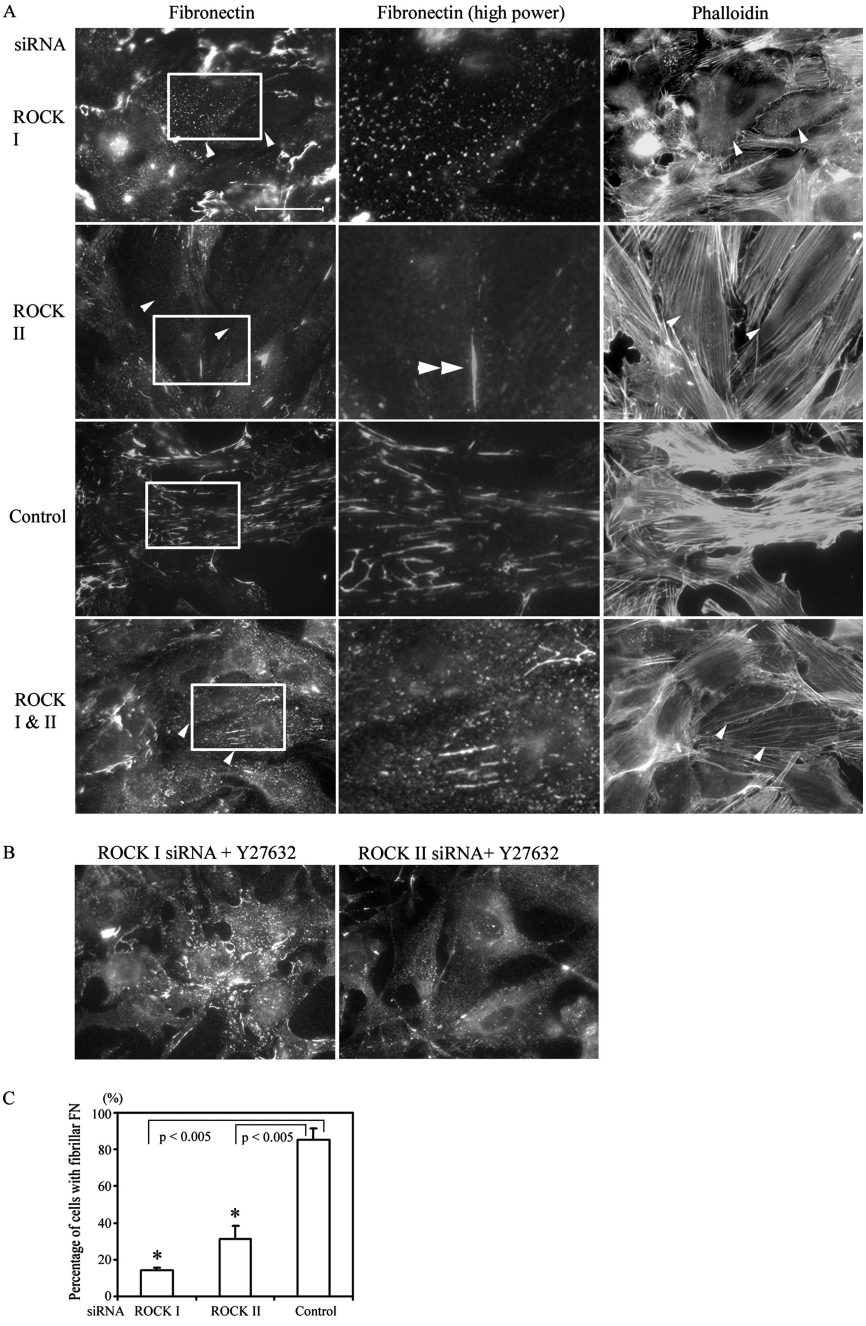

Figure 2. ROCKs I and -II are required for FN matrix assembly. (A) REFs were transfected with ROCK I, ROCK II, control, or a mixture of ROCK I and -II siRNAs. After 2 d, REFs were fixed and stained for FN and F-actin. All siRNA-transfected cells are arrowed. High-power micrographs (2.7× magnification) show corresponding areas boxed in the left micrographs. Double arrowheads indicate stitches in ROCK II-deficient cells. (B) REFs were treated with ROCK I or ROCK II siRNAs for 2 d and then treated with 30 μM Y-27632 for 4.5 h, fixed, and stained for FN. Bar, 50 μm. (C) Quantitation of cells with fibrillar FN in ROCK-deficient REFs compared with control REF. The average of three independent experiments is shown, and error bars indicate SEM. Asterisks denote a significant difference.

Deoxycholate (DOC) Lysis

REFs were washed with Tris-buffered saline, and FN matrix was solubilized using 100 μl of DOC lysis buffer as described previously (Sechler *et al.*, 1996). After centrifugation, the DOC-insoluble pellet was solubilized in 10 μl of SDS sample buffer in the presence of a reducing reagent. Equal volumes of DOC-insoluble samples were analyzed by 7.5% SDS-PAGE. Samples were immunoblotted with R2/7 antibodies. DOC-soluble samples were immunoblotted in parallel with antibodies against actin as loading controls.

Metabolic Labeling

Forty-eight hours after siRNA transfection, REFs in 24-well plates were incubated in Met/Cys-free DMEM (Invitrogen) with 5% FN-depleted and -dialyzed FCS and 20 μCi of [^{35}S]Met/Cys ProMIX (>1000 Ci/mM; GE Healthcare, Little Chalfont, Buckinghamshire, United Kingdom) for 5 h. Metabolically labeled FN in conditioned medium was immunoprecipitated with R2/7 antibodies on protein A-Sepharose (GE Healthcare) for 1 h at room temperature. Nearly complete immunoprecipitation was confirmed by the absence of FN in the supernatants after immunoprecipitation. Beads were washed with buffer (50 mM Tris-Cl, pH 7.6, 150 mM NaCl, 1% Triton X-100, 0.5% DOC, and 0.1% SDS) four times. Immunoprecipitates were separated by 7.5% SDS-PAGE, FN polypeptides were excised, and their radiolabel content was analyzed by scintillation counter and normalized by cell number.

Reverse Transcription-PCR

One microgram of total RNA isolated from each siRNA-transfected cell culture was reverse transcribed by avian myeloblastosis virus reverse transcriptase (Promega, Madison, WI) and oligo(dT)$_{15}$ primer. PCR were carried out by KOD Hot Start DNA polymerase, mixtures of reverse transcripts and primers as shown below. To amplify EIIIA variants of rat cellular FN, primers were 5′-TTGCAACCCACCGTGGAGTATGTG and 5′-CTCGGTAGC CAGTGAGCTTAACAC; for EIIIB, 5′-GGTTCATGCCGATCAGAGTTCCTGC and 5′-AGAGGTTGGTTAGCTCAATGGACG; for V, 5′-TGGTGTCAC GGAGGCCACCATCACT and 5′-AGTGCCAACAGGTTGGCATGAAATG. After 94°C for 2 min to activate polymerase, EIIIA and EIIIB were amplified by 94°C for

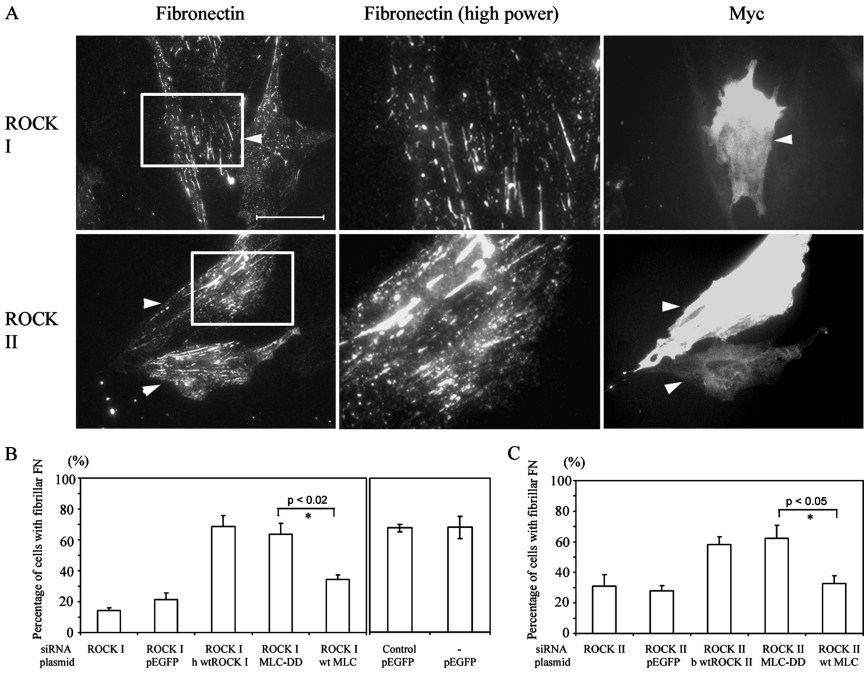

Figure 3. FN matrix assembly defects in ROCK-deficient REF were rescued by expression of corresponding wild-type rho kinases. (A) REFs were cotransfected with Cy3-labeled ROCK siRNAs and myc-wild type human ROCK I or bovine ROCK II. After 2 d, cells were fixed and stained for FN and myc epitope. Arrowheads show double-transfected cells. High-power micrographs (2.7× magnification) in the center show corresponding areas boxed in the left micrographs. Bar, 50 μm. (B and C) Quantitation of cells with fibrillar FN. REFs were cotransfected with ROCK I or -II siRNA with wtROCK I or -II cDNA as appropriate, MLC-DD-GFP or MLCwt-GFP cDNA, and pEGFP plasmid and/or control siRNA. The mean of three independent experiments and error bars (SEM) is shown. Asterisks denote a significant difference. Data for ROCK I- or -II–depleted cells were taken from Figure 2C.

30 s, 50°C for 30 s, and 72°C for 60 s for 35 cycles, and V by 94°C for 30 s, 60°C for 30 s, and 72°C for 60 s for 37 cycles.

Pull-Down Assay

Pull-down assay for GTP-loaded Cdc42 was performed according to Ren *et al.* (1999). The signals from Western blotting were analyzed by NIH Image version 1.61.

FN-coated Beads-binding Assay

FN-coated latex red beads (average bead size 1.0 μm) were prepared as described previously (Yoneda *et al.*, 2005). Control beads were coated with BSA alone. Control or siRNA-transfected cells were incubated at 4°C for 10 min, and then $\sim 9 \times 10^9$ FN-coated beads were added. Cells were further incubated at 4°C for 30 min to allow beads to interact with the cell surface and then incubated at 37°C for 1 h. After washing cells were fixed with 4% PFA. Numbers of beads associated with cells were counted. Specificity of this assay was confirmed by the control beads that were removed in the washing steps.

RESULTS

ROCK I or -II Deletion Blocks FN Matrix Assembly

To examine whether actomyosin contractility and RhoA/ROCK pathway are required for FN matrix assembly, freshly seeded primary fibroblasts were treated with various inhibitors of RhoA and myosin II function for 16 h. FN matrix assembly proceeds rapidly in confluent fibroblasts, but it was substantially blocked by the C3 transferase inhibitor (Wilde and Aktories, 2001) of RhoA, and the myosin II inhibitor blebbistatin (Figure 1; Limouze *et al.*, 2004). It was also blocked by Y-27632, a specific inhibitor of both ROCK I and -II (Ishizaki *et al.*, 2000) in REFs. FN matrix assembly was limited to small aggregates of FN on the cell surface, either punctate or short fibrils (Figure 1). Specific inhibition of each ROCK by siRNA revealed a further complexity. Down-regulation of ROCK I gave a similar result to Y-27632, there being just a few small patches of cell surface FN (Figure 2A). Absence of ROCK II revealed a different defect; whereas FN matrix assembly was much reduced compared with a control siRNA treatment or no treatment, the FN was present as "stitches" between cells or between cells and the substrate (Figure 2A). Numbers of cells with fibrillar FN were significantly attenuated after ROCK I or ROCK II depletion compared with controls (Figure 2C). The same phenotypes were observed in the absence or presence of exogenous FN from plasma (Supplemental Figure 1).

As before (Yoneda *et al.*, 2005), ROCK I depletion by siRNA led to loss of microfilament bundles (Figure 2A) and focal adhesions, despite unchanged levels of ROCK II proteins. Similarly, loss of ROCK II gave rise to a flattened phenotype with exaggerated stress fibers and focal adhesions (Figure 2A; Yoneda *et al.*, 2005); these actin-containing structures were ROCK I dependent and were correspondingly lost from ROCK II siRNA-treated cells either by treatment with Y-27632 ROCK inhibitor, or cotransfection with ROCK I siRNA (Figure 2A). In ROCK II siRNA, followed by Y-27632 treatment, FN matrix assembly was greatly diminished, with only apical punctate patches, resembling those of ROCK I-depleted cells, remaining (Figure 2, A and B). Therefore, although loss of FN matrix correlated with disruption of stress fibers in the case of ROCK I suppression, it did not where ROCK II was depleted. As controls for these experiments, coexpression of full-length wild-type ROCK I or -II cDNAs along with the corresponding siRNA oligonucleotides corrected the phenotype, with copious FN matrix deposition (Figure 3). In this case, human ROCK I and bovine ROCK II cDNAs were transfected into the rat cells, to avoid their down-regulation by the siRNA treatments. In addition, control siRNA-treated cells showed no loss of either ROCK protein (Yoneda *et al.*, 2005) or altered FN matrix (Figure 2, A and C).

It is known that as FN matrix matures, it becomes progressively insoluble in DOC (McKeown-Longo and Mosher, 1983). Secreted FN is initially 2% DOC soluble, whereas fibrillar FN is insoluble. To examine the state of cell-associated FN in ROCK I- and ROCK II–deficient cells, DOC detergent solubility was analyzed. Treatment of REF cultures depleted of ROCK I with DOC almost completely solubilized the punctate FN, indicating that the maturation steps of covalent cross-linking had not taken place (Figure 4, A–C). In contrast, some DOC insoluble FN was observed in

ROCK II-depleted cells, but this pool was more abundant in control siRNA-treated cultures, with a ratio of control: ROCK II depleted = 1:0.45 ± 0.03 when normalized to actin (data indicates mean ± SEM, n = 3, $p < 0.005$). The L8 monoclonal antibody inhibits FN matrix assembly (Chernousov *et al*., 1987) and detects an FN epitope in the I_9–III_1 region (Chernousov *et al*., 1991) only revealed by tension and therefore dependent on the state of cell contractility (Zhong *et al*., 1998). Some colocalization of L8 antibody and polyclonal FN antibody patterns was observed in both ROCK I- and -II–deficient cells (Supplemental Figure 2). Therefore, some cell surface FN in ROCK I- and -II–deficient cells is in an extended form as recognized by L8 antibody. In a further control experiment, it was noted that L8 antibody staining was minimal in the remnant FN matrix present in blebbistatin-treated REF monolayers (Supplemental Figure 2). Additional experiments with DOC solubility and L8 staining also showed that the effects of rho kinase loss were not transient or a result of slowed FN matrix assembly (data not shown).

No Impairment of FN Synthesis, Stability, or α5β1 Integrin Function Results from the Absence of the Rho Kinases, and Tensin Demarcates FN Matrix Assembly Points

One possible reason for the lack of FN matrix in ROCK-depleted cells was a lack of synthesis and/or export. However, metabolically labeled FN could be immunoprecipitated from culture media where either ROCK I or -II had been reduced by siRNA treatments. ROCK I-deficient cells secreted more FN into culture medium than either ROCK II-deficient or control cells (Figure 4D). Moreover, the FN was detectable as full length in the cell-associated (Figure 4, A–C) and conditioned medium pools (data not shown), with M_r ~250 kDa under reducing conditions. This indicated there were no obvious proteolytic activity differences in the various conditions. As a further control for cell surface metalloproteinase activity, such as matrix metalloproteinases (MMPs), membrane type-MMPs or ADAMs, cultures were treated with 10 μM GM6001 hydroxamate inhibitor (Galardy *et al*., 1994) for 48 h after transfection. This did not restore FN matrix assembly where ROCK I or -II had been depleted, and it seemed not to affect FN matrix assembly in control cultures either (Supplemental Figure 3). In separate experiments, this level of GM6001 was shown to block receptor shedding from murine epithelial cells (Mahalingam, Nagase, and Couchman, unpublished data).

In further experiments, the alternate splicing characteristics of the FN synthesized by control or siRNA-treated fibroblasts were examined. Rat FN splicing variants include the insertion of an additional exon, EIIIA and/or EIIIB, and three alternative splicing V variants (V0, V95, and V120) (equivalent to the IIICS domain in humans; Tamkun *et al*., 1984). Splicing patterns are regulated during development and aging (Pagani *et al*., 1991), and it has been suggested that $EIIIB^{-/-}$ cells in culture have reduced FN matrix assembly (Fukuda *et al*., 2002), whereas the V region is essential for FN dimer secretion (Schwarzbauer *et al*., 1989). Three sets of primers were used to determine the presence or absence of EIIIA, EIIIB, and the pattern of V splicing. The results were in each case the same (Supplemental Figure 4), with the detection of EIIIA+ and − variants, two variants of IIICS (V95 and V120 but not V0), and the apparent absence of EIIIB. Therefore, the failure to establish FN matrix in ROCK I-depleted cells, or its maturation in the case of ROCK II-depleted cells, could not be ascribed to changes in splicing pattern that might affect self-association of FN dimers.

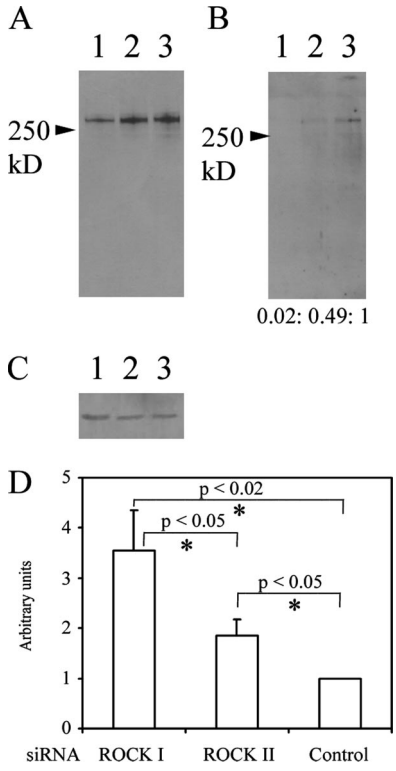

Figure 4. Small patches of FN in ROCK I-deficient cells are DOC soluble, but FN synthesis is not reduced by siRNA treatment. REFs were transfected with ROCK I (lanes 1), ROCK II (lanes 2), and control (lanes 3) siRNAs and after 2 d, cells were lysed with 2% DOC buffer. Lysates were separated into DOC-soluble (A) and -insoluble (B) pools as described in *Materials and Methods*. Both fractions were subjected to FN Western blotting (A and B). Numbers in B represent blot quantitation after normalization with actin. (C) For loading controls, the DOC-soluble fractions were also analyzed for actin content. (D) REFs transfected with siRNA for 48 h were metabolically labeled with [^{35}S Met/Cys] for a further 5 h. Culture media were collected and secreted FN was immunoprecipitated, resolved by SDS-PAGE, and radiolabel contents were measured. Radiolabeled FN quantitation was normalized by cell number from parallel cultures. Data are shown relative to that of control cells. Error bars indicate SEM (n = 4). Asterisks denote a significant difference.

Also known to be a critical early step in FN matrix assembly is binding to the α5β1 integrin (McDonald *et al*., 1987; Fogerty *et al*., 1990), abundant in control fibroblasts. Cell surface staining for α5 and β1 integrin showed similar patterns to FN whether a ROCK was depleted or not (Supplemental Figure 5, A and B), suggesting that remnant FN associated with this integrin. Moreover, control and ROCK siRNA-treated cells could attach and spread on both FN and a 110-kDa central cell-binding domain ($III_{3–11}$) of FN (Supplemental Figure 5, C and D), arguing that the α5β1 integrin was active in all cases. Because cell surface FN receptors other than integrin α5β1 might be affected in rho kinase-depleted fibroblasts, the overall ability of FN binding at cell surface was analyzed. FN-coated fluorescent 1.0-μm beads were added to cultures. Comparable numbers of beads (average 8.6 beads/cell in ROCK I-depleted cells (n = 20), 10.2/cell in ROCK II depletion (n = 22), and 7.0/cell in control cells (n = 21) were associated with cells in each case, again indicating no impairment in FN interactions with cell surfaces where ROCKs had been depleted. It should be noted that ROCK II-depleted cells have increased spread cell

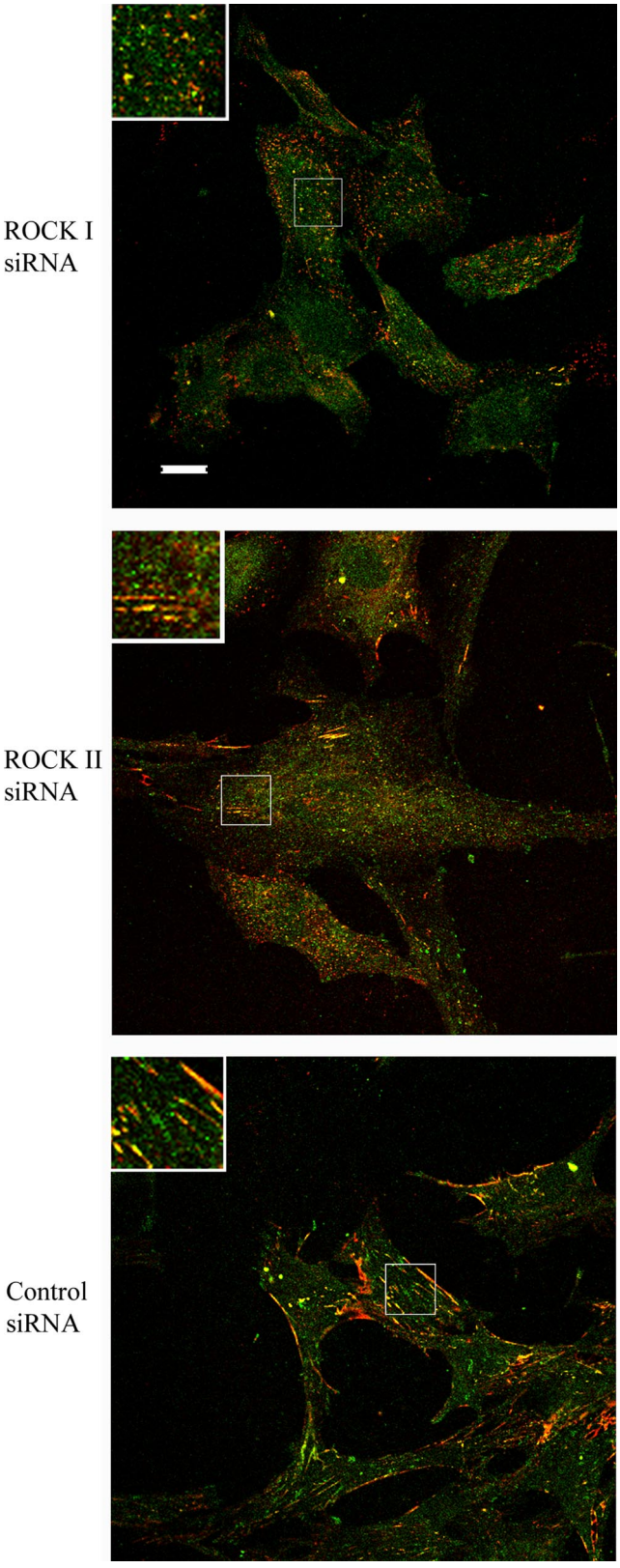

Figure 5. FN partially localizes to tensin-rich sites in ROCK-deficient REFs. siRNA-transfected REFs were fixed and stained for tensin (green) and FN (red). Images were acquired by laser scanning confocal microscopy. The inserts are magnified images of the boxed areas. Bar, 20 μm.

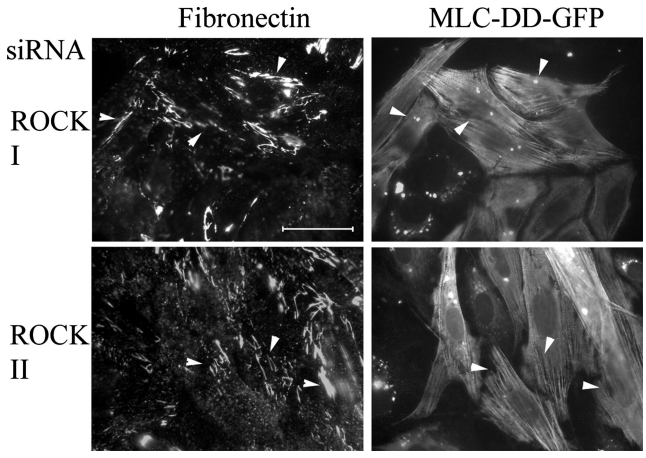

Figure 6. FN matrix assembly defect in ROCK-deficient REF was rescued by the expression of phosphomimetic form of MLC-GFP. REFs stably expressing phosphomimetic form of MLC-GFP were transfected with Cy3-labeled ROCK siRNAs. Cells were stained for FN. All double transfected cells are arrowed. Bar, 50 μm. Quantitation of these data are shown in Figure 3, B and C. High-power micrographs (2.7× magnification) in the center show corresponding areas boxed in the left micrographs.

surface area over ROCK I-depleted or control cells (Yoneda *et al.*, 2005).

Consistent with the presence of functional $\alpha5\beta1$ integrin, confocal microscopic analysis showed that the actin-associated protein tensin partially colocalized at the cell surface with FN in all cases (Figure 5). Where ROCK I was diminished by siRNA, tensin staining was punctuate, whereas the short linear streaks of FN in ROCK II-depleted cells was complemented by closely similar tensin staining. Where a florid FN matrix was present in control siRNA-treated cultures, tensin colocalized at the cell surface with a subset of FN matrix fibrils. Therefore, the association of tensin in submembranous concentrations, colocalized with FN, is apparently unrelated to the presence or absence of microfilament bundles. The data also further suggest the initiation of FN matrix assembly, but a failure of maturation, where either ROCK was down-regulated.

FN Matrix Restoration by Phosphomimetic MLC

One of major substrates of the two rho kinases is MLC, which is phosphorylated on Thr18 and Ser19 (Amano *et al.*, 1996). Previously, we have shown a substantial reduction in such phosphorylation in ROCK I- but not ROCK II-depleted cells (Yoneda *et al.*, 2005). To establish whether phosphorylated MLC is a key participant in FN matrix assembly, REF stably expressing a phosphomimetic form of MLC (Thr18→Asp, Ser19→Asp; MLC-DD) fused to GFP was transfected with ROCK I or ROCK II siRNAs. MLC-DD-GFP expression corrected the FN matrix assembly phenotype of ROCK depletion, and MLC-DD was incorporated into stress fibers (Figure 6). FN matrix assembly was restored in both ROCK I- and -II–depleted cells, to levels equivalent to controls (i.e., enhanced GFP ± control siRNA transfection). Quantification is shown in Figure 3, B and C. All this suggests that a common downstream molecule regulating myosin II is required. In further control experiments, expression of wild-type MLC-GFP did not restore the FN matrix defect in ROCK II-deficient cells, whereas some recovery, but still less fibrillar FN compared with MLC-DD expression, was observed in ROCK I-deficient cells (Figure 3, B and C). The

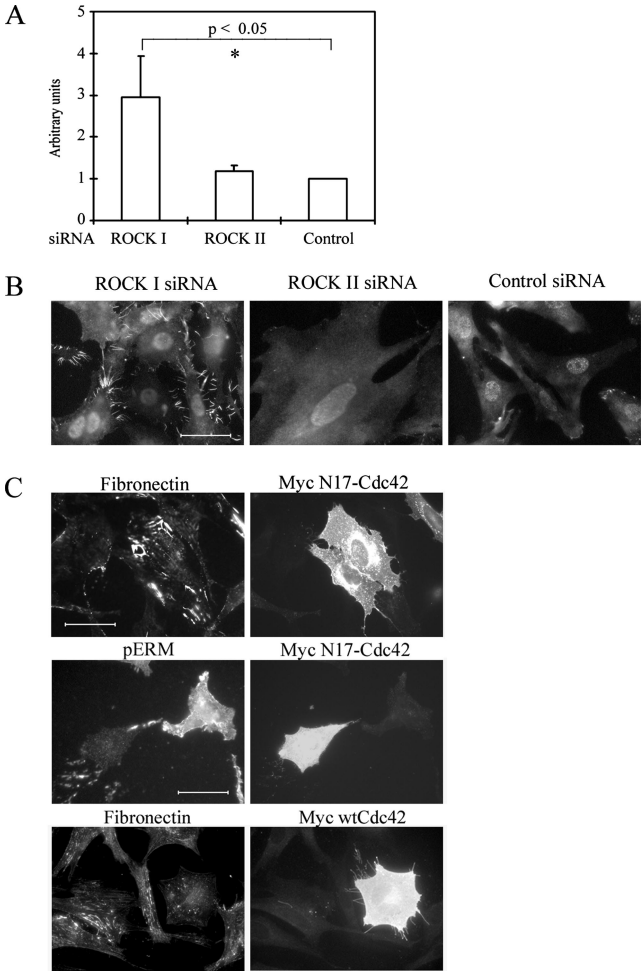

Figure 7. Surface morphology of ROCK I-deficient REFs affects FN matrix assembly. (A) GTP–Cdc42 levels in siRNA-transfected REFs were analyzed by PAK-CRIB pull-down assays. Relative amounts of GTP-Cdc42 were compared with data from control siRNA transfectant. Error bars indicate SEM (n = 4). Asterisks denote a significant difference. (B) siRNA-transfected REF were fixed and stained for phospho-ERM proteins. Bar, 50 μm. (C) REFs were cotransfected with Cy3-labeled ROCK I siRNA and myc-N17-Cdc42 plasmid. After 2 d, cells were fixed and stained for myc epitope and phospho-ERM or FN. In control experiments, REFs were transfected with myc-wild type-Cdc42 plasmid. After 2 d, cells were fixed and stained for FN and myc epitope. Bar, 50 μm.

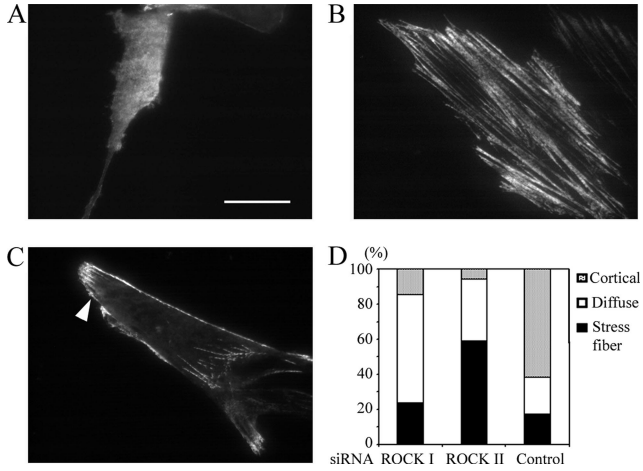

Figure 8. MLC localization is altered in ROCK-deficient REF cells. REFs were cotransfected with siRNA and wild-type MLC-GFP and incubated for 2 d. Localization of MLC-GFP within 100 nm of the substrate in living cells was analyzed by TIRF microscopy. Three types of localization were observed: diffuse membranous distribution in ROCK I-deficient REF cells (A), associated with stress fibers in ROCK II-deficient REF cells (B), and localized cortical areas in control REFs (C). In control cells, stress fiber localizations are not visible due to characteristics of TIRF, but adhesion structures are visible. Arrowhead denotes visible adhesion structure. Quantitation of the three types is shown for each siRNA treatment (D) (n = 34 for ROCK I siRNA and ROCK II siRNA and 29 for control siRNA). Bar, 20 μm.

fact that expression of MLC-DD in ROCK II siRNA-treated cells led to restored FN matrix, despite the presence of phosphorylated MLC in stress fibers of ROCK II-depleted cells (Yoneda *et al*., 2005), suggests that FN matrix assembly requires a myosin II-driven process other than stress fiber formation.

FN Matrix Loss Resulting from ROCK I Depletion Was Secondary to Cdc42 Activity

Lysophosphatidic acid treatment of fibroblasts, leading to increased GTP-RhoA levels in turn resulted in enhanced FN matrix assembly (Zhang *et al*., 1997). Therefore, to determine whether the loss of ROCKs in turn led to a reduction in GTP-RhoA levels, conventional pull-down assays (Ren *et al*., 1999) were performed on control siRNA-treated cells and those depleted of ROCK I or -II by siRNA. The results showed that in all cases, GTP-RhoA and GTP-Rac1 were present and not greatly changed from untreated controls (Yoneda *et al*., 2005). Moreover, lysophosphatidic acid in serum was not able to restore FN matrix assembly in cells lacking ROCK I or -II. With respect to levels of GTP-Cdc42, however, a large increase was seen in cells lacking ROCK I, compared with control siRNA treatment (Figure 7A). This was also observed in Rat1 fibroblasts (a mean 2.8-fold increase). Because Cdc42 is known to induce filopodial structures (Etienne-Manneville and Hall, 2002), accompanied by phosphorylation of ezrin/radixin/moesin (ERM) proteins (Nakamura *et al*., 2000), we examined whether ROCK I-deficient cells show those structures. The presence of many filopodial structures enriched in phosphorylated ERM proteins were observed in ROCK I siRNA cultures, and these were less conspicuous in either ROCK II or control siRNA cultures (Figure 7B). To ascertain whether elevated GTP-Cdc42 might be responsible for the lack of FN matrix assembly, we performed two experiments. The first was cotransfection of ROCK I siRNA with dominant-negative Cdc42 cDNA, whereas the second was promotion of filopodial structure by overexpressing wild-type Cdc42 cDNA in normal fibroblasts. Cotransfection experiments led to a recovery of FN matrix assembly (Figure 7C) that was qualitatively indistinguishable from untreated control cultures. Overexpression of wild-type Cdc42 indeed induced filopodial structures and disrupted FN matrix assembly (Figure 7C). Increased levels of GTP-Cdc42 suppress FN matrix assembly, suggesting that the defect in ROCK I-deficient cells was secondary to a change in cell surface architecture.

Most Submembranous MLC in ROCK II-deficient Fibroblasts Is Incorporated into Stress Fibers

Overexpression of MLC-DD restored FN matrix assembly in both ROCK I- and -II–depleted cells, despite the presence of phospho-MLC in stress fibers in the latter case. This sug-

gested that a membrane-associated pool of MLC is important for FN matrix assembly. Furthermore, alteration of surface morphology by GTP-Cdc42 reduction in ROCK I-deficient cells also restored FN matrix assembly. Therefore, the possibility that submembranous actomyosin organization might be altered in ROCK-deficient fibroblasts was investigated. TIRF microscopic analysis (for review, see Toomre and Manstein, 2001) was carried out to observe the submembranous distribution of wild-type MLC in living fibroblasts. Three different distributions of MLC-GFP were observed: a diffuse distribution (Figure 8A), a distribution incorporated into stress fibers (Figure 8B), and a distribution in cortical microfilaments (Figure 8C). A majority of ROCK II-deficient cells had MLC incorporated into stress fibers only (Figure 8D), whereas ROCK I deficiency led to a mostly diffuse membranous distribution. Control cells had a dominant cortical distribution as well as adhesion structures. These results suggested that in both cases of ROCK depletion, REFs had an altered membrane-association of MLC. In particular, MLC restricted to stress fibers is apparently not commensurate with FN matrix assembly. Supporting this, the expression of MLC-DD-GFP restored the cortical localization of MLC (data not shown) as well as FN matrix in ROCK II-depleted cells (Figure 3C).

DISCUSSION

Extracellular and intracellular parameters are known to be important in FN matrix assembly (Mao and Schwarzbauer, 2005). It is an active, cell-driven process in which the integrin $\alpha5\beta1$ is a major contributor and a starting point for FN binding. Roles for the cytoskeleton emerged through work with cytochalasin B (Kurkinen *et al*., 1978), cytochalasin D (Cario-Toumaniantz *et al*., 2002), and inhibitors of Rho GTPase (Zhang *et al*., 1997). Force may need to be applied to FN molecules, which may have some elastic properties, so that they unfold and present self-association sites for FN matrix formation on the cell surface (Zhong *et al*., 1998). Although lysophosphatidic acid working through a seven membrane spanning receptor and csk to elevate GTP-Rho A levels (Lowry *et al*., 2002) promoted FN matrix assembly, the downstream effectors were not elucidated. In this report, further components are apparent. The rho kinase substrate MLC is required for extracellular FN matrix assembly. This is entirely consistent with a force-generating role of myosin II and our results with blebbistatin, Tat-C3, and Y-27632 rho kinase inhibitor. However, results from rho kinase siRNA treatments require careful evaluation. In the absence of ROCK I, almost no FN matrix assembly took place, there being small punctuate deposits on the cell surface but no sign of fiber assembly. In contrast, the absence of ROCK II did not prevent FN matrix initiation on the cell surface or the establishment of some DOC insolubility, but there was no progression beyond this point. Levels of GTP-Cdc42 were elevated significantly as a result of ROCK I depletion. Although the molecular basis for this is not known, it resembles previous findings that inhibition of both rho kinases through Y-27632 treatment leads to increased GTP-Rac1 levels in a Rho-dependent manner (Tsuji *et al*., 2002), although not seen here. As expected from high GTP–Cdc42 levels, many filopodia rich in phosphorylated ERM proteins were present. This disturbance in cell surface architecture seems to be responsible for a lack of FN matrix, because transfection of a dominant negative Cdc42 construct restored FN matrix assembly even in the continued absence of ROCK I protein. Furthermore, induction of filopodial structures through overexpression of wild-type Cdc42 in control cells resulted in loss of FN matrix. Therefore, although both rho kinases affect FN matrix assembly, their contributions are different. It should be noted that ROCK II levels persisted when ROCK I was down-regulated by siRNA, and vice versa (Yoneda *et al*., 2005).

Using the same siRNA protocols as here, we determined previously that ROCK I was necessary for the assembly of microfilament bundles and focal adhesions (Yoneda *et al*., 2005). ROCK II depletion enhanced microfilament bundles and focal adhesion formation. However, the internalization of small FN-coated beads was compromised in the absence of ROCK II but not ROCK I. This indicated that myosin II populations for microfilament bundle assembly and FN matrix internalization are distinct, as are stress fiber formation and FN matrix assembly as shown here. This is emphasized by expression of phosphomimetic MLC that reestablished FN matrix assembly even in the absence of ROCK II and where stress fibers decorated with phospho-MLC persist (Yoneda *et al*., 2005). The data as a whole therefore indicate that a pool of MLC distinct from that associated with ROCK I-promoted stress fibers is required for FN matrix assembly. TIRF microscopy is a powerful method to examine cytoskeletal structures <100 nm from the substrate (Toomre and Manstein, 2001). This showed a clear difference in the organization of MLC in siRNA-treated living cells. In ROCK II-depleted REFs, stress fibers were dominant, but they were less obvious in other treatments. The data suggest that a submembranous pool of myosin II under ROCK II regulation is required for FN matrix assembly but that it can be bypassed by phosphomimetic MLC expression. Initiation of FN matrix assembly requires a functional actin cytoskeleton other than stress fibers and there may be a relationship between the ability to internalize FN and the ability to assemble a mature extracellular FN matrix. Clustering and internalization, or endocytic mechanisms, may be related to the establishment of extracellular FN matrix on the cell surface (Lyubimov and Vasiliev, 1982) and that is supported by the data here.

Depletion of integrin-linked kinase by siRNA suppressed FN matrix assembly (Vouret-Craviari *et al*., 2004), and the extent and persistence of RhoA activation were reduced during cell spreading compared with controls. Effects of integrin-linked kinase depletion could therefore be partially mediated by reduced rho kinase activities. Regulation of the two rho kinases may be separable because the PH domains of the two rho kinases are somewhat dissimilar and have different phospholipid-binding profiles. ROCK II function may be regulated in part by the phosphatidylinositol-3 kinase pathway (Yoneda *et al*., 2005), and relationships between this pathway and FN fiber assembly are not well understood, although phosphatidylinositol-3 kinase activity may be required for initiation of assembly (Wierzbicka-Patynowski and Schwarzbauer, 2002).

Control experiments indicated that FN synthesis was not compromised by the absence of either ROCK I or -II, and the alternate splicing profile of the FN mRNA was unchanged. There was also no evidence of enhanced proteolytic activity in the absence of either rho kinase. A FN matrix is required very early in vertebrate development (George *et al*., 1993), as is $\beta1$ integrin (Fässler and Meyer, 1995), yet the ROCK II knockout mouse clearly develops much further, although it does have a clear and pronounced phenotype (Thumkeo *et al*., 2003). Few ROCK $I^{-/-}$ mice survive to late development or birth (Zhang *et al*., 2006) consistent with other in vivo evidence suggesting that ROCKs I and -II are not redundant (Rikitake *et al*., 2005; Thumkeo *et al*., 2005). However, it seems that some compensatory mechanisms may contribute

to FN matrix assembly in vivo that cannot be elicited under culture conditions where levels of one protein are acutely reduced or eliminated. Supporting a function for rho kinases in FN matrix assembly, ROCK I heterozygous mice (Rikitake *et al*., 2005) and ROCK I homozygous null mice (Zhang *et al*., 2006) showed attenuated perivascular fibrosis in response to angiotensin II treatment or pressure overload. Because perivascular fibrosis is likely derived from fibroblastic cells, the data are consonant with roles for rho kinases in FN matrix assembly both in vitro and in vivo. Rho kinase activity may also be an important component of the pathogenesis of fibrotic disease.

In conclusion, the two rho kinases have separable roles in terms of actin cytoskeleton and FN matrix assembly regulation. ROCK I is required for microfilament bundle and focal adhesion assembly, and our data further suggest that ROCK II has a distinct and necessary role in the establishment of a mature FN fibrillar matrix.

ACKNOWLEDGMENTS

We thank A. Hall, S. Narumiya, K. Kaibuchi, J. Bertoglio, M. A. Chernousov, and V. Braga for gifts of antibodies and cDNAs. We thank laboratory members for help and advice. This work was supported by Program Grant 065940 from the Wellcome Trust (to J.R.C.) and the Interdisciplinary Research Centre in Bionanotechnology from The Engineering and Physical Sciences Research Council (to D.U.).

REFERENCES

Amano, M., Ito, M., Kimura, K., Fukata, Y., Chihara, K., Nakano, T., Matsuura, Y., and Kaibuchi, K. (1996). Phosphorylation and activation of myosin by Rho-associated kinase (Rho-kinase). J. Biol. Chem. *271*, 20246–20249.

Baneyx, G., Baugh, L., and Vogel, V. (2002). Fibronectin extension and unfolding within cell matrix fibrils controlled by cytoskeletal tension. Proc. Natl. Acad. Sci. USA *99*, 5139–5143.

Bishop, A. L., and Hall, A. (2000). Rho GTPases and their effector proteins. Biochem. J. *348*, 241–255.

Burridge, K., and Wennerberg, K. (2004). Rho and Rac take center stage. Cell *116*, 167–179.

Cario-Toumaniantz, C., Evellin, S., Maury, S., Baron, O., Pacaud, P., and Loirand, G. (2002). Role of rho kinase signalling in healthy and varicose human saphenous veins. Br. J. Pharmacol. *137*, 205–212.

Chernousov, M. A., Faerman, A. I., Frid, M. G., Printseva, O. Y., and Koteliansky, V. E. (1987). Monoclonal antibody to fibronectin which inhibits extracellular matrix assembly. FEBS Lett. *217*, 124–128.

Chernousov, M. A., Fogerty, F. J., Koteliansky, V. E., and Mosher, D. F. (1991). Role of the I-9 and III-1 modules of fibronectin in formation of an extracellular fibronectin matrix. J. Biol. Chem. *266*, 10851–10858.

Etienne-Manneville, S., and Hall, A. (2002). Rho GTPases in cell biology. Nature *420*, 629–635.

Fässler, R., and Meyer, M. (1995). Consequences of lack of beta 1 integrin gene expression in mice. Genes Dev. *9*, 1896–1908.

Fogerty, F. J., Akiyama, S. K., Yamada, K. M., and Mosher, D. F. (1990). Inhibition of binding of fibronectin to matrix assembly sites by anti–integrin (alpha5beta1) antibodies. J. Cell Biol. *111*, 699–708.

Fukuda, T., Yoshida, N., Kataoka, Y., Manabe, R., Mizuno-Horikawa, Y., Sato, M., Kuriyama, K., Yasui, N., and Sekiguchi, K. (2002). Mice lacking the EDB segment of fibronectin develop normally but exhibit reduced cell growth and fibronectin matrix assembly in vitro. Cancer Res. *62*, 5603–5610.

Galardy, R. E., *et al*.. (1994). Low molecular weight inhibitors in corneal ulceration. Ann. NY Acad. Sci. *732*, 315–323.

George, E. L., Georges-Labouesse, E. N., Patel-King, R. S., Rayburn, H., and Hynes, R. O. (1993). Defects in mesoderm, neural tube and vascular development in mouse embryos lacking fibronectin. Development *119*, 1079–1091.

Ishizaki, T., Uehata, M., Tamechika, I., Keel, J., Nonomura, K., Maekawa, M., and Narumiya, S. (2000). Pharmacological properties of Y-27632, a specific inhibitor of rho-associated kinases. Mol. Pharmacol. *57*, 976–983.

Katz, B-Z., Zamir, E., Bershadsky, A., Kam, Z., Yamada, K. M., and Geiger, B. (2000). Physical state of the extracellular matrix regulates the structure and molecular composition of cell-matrix adhesions. Mol. Biol. Cell *11*, 1047–1060.

Klass, C. M., Couchman, J. R., and Woods, A. (2000). Control of extracellular matrix assembly by syndecan-2 proteoglycan. J. Cell Sci. *113*, 493–506.

Kurkinen, M., Wartiovaara, J., and Vaheri, A. (1978). Cytochalasin B releases a major surface-associated glycoprotein, fibronectin, from cultured fibroblasts. Exp. Cell Res. *111*, 127–137.

Limouze, J., Straight, A. F., Mitchison, T., and Sellers, J. R. (2004). Specificity of blebbistatin, an inhibitor of myosin II. J. Muscle Res. Cell Motil. *25*, 337–341.

Lowry, W. E., Huang, J., Ma, Y.-C., Ali, S., Wang, D., Williams, D. M., Okada, M., Cole, P. A., and Huang, X.-Y. (2002). Csk, a critical link of G protein signals to actin cytoskeletal reorganization. Dev. Cell *2*, 733–744.

Lyubimov, A. V., and Vasiliev, J. M. (1982). Distribution of fibronectin-containing structures on the surface of lamelloplasm and endoplasm of fibroblasts; hypothesis of receptor-mediated assembly of fibronectin structures. Cell Biol. Int. Rep. *6*, 105–112.

Mao, Y., and Schwarzbauer, J. E. (2005). Fibronectin fibrillogenesis, a cell-mediated matrix assembly process. Matrix Biol. *24*, 389–399.

McCarthy, K. J., Bynum, K., St. John, P. L., Abrahamson, D. R., and Couchman, J. R. (1993). Basement membrane proteoglycans in glomerular morphogenesis: chondroitin sulfate proteoglycan is temporally and spatially restricted during development. J. Histochem. Cytochem. *41*, 401–414.

McDonald, J. A., Quade, B. J., Broekelmann, T. J., LaChance, R., Forsman, K., Hasegawa, E., and Akiyama, S. (1987). Fibronectin's cell-adhesive domain and an amino-terminal matrix assembly domain participate in its assembly into fibroblast pericellular matrix. J. Biol. Chem. *262*, 2957–2967.

McKeown-Longo, P. J., and Mosher, D. F. (1983). Binding of plasma fibronectin to cell layers of human skin fibroblasts. J. Cell Biol. *97*, 466–472.

Nakamura, N., Oshiro, N., Fukata, Y., Amano, M., Fukata, M., Kuroda, S., Matsuura, Y., Leung, T., Lim, L., and Kaibuchi, K. (2000). Phosphorylation of ERM proteins at filopodia induced by Cdc42. Genes Cells *5*, 571–581.

Pagani, F., Zagato, L., Vergani, C., Casari, G., Sidoli, A., and Baralle, F. E. (1991). Tissue-specific splicing pattern of fibronectin messenger RNA precursor during development and aging in rat. J. Cell Biol. *113*, 1223–1229.

Ren, X.-D., Kiosses, W. B., and Schwartz, M. A. (1999). Regulation of the small GTP-binding protein Rho by cell adhesion and the cytoskeleton. EMBO J. *18*, 578–585.

Rikitake, Y., Oyama, N., Wang, C. Y., Noma, K., Satoh, M., Kim, H. H., and Liao, J. K. (2005). Decreased perivascular fibrosis but not cardiac hypertrophy in ROCK1+/− haploinsufficient mice. Circulation *112*, 2959–2965.

Schwarzbauer, J. E., Spencer, C. S., and Wilson, C. L. (1989). Selective secretion of alternatively spliced fibronectin variants. J. Cell Biol. *109*, 3445–3453.

Sebbagh, M., Renvoizé, C., Hamelin, J., Riché, N., Bertoglio, J., and Bréard, J. (2001). Caspase-3-mediated cleavage of ROCK I induces MLC phosphorylation and apoptotic membrane blebbing. Nat. Cell Biol. *3*, 346–352.

Sechler, J. L., Takada, Y., and Schwarzbauer, J. E. (1996). Altered rate of fibronectin matrix assembly by deletion of the first type III repeats. J. Cell Biol. *134*, 573–583.

Tamkun, J. W., Schwarzbauer, J. E., and Hynes, R. O. (1984). A single rat fibronectin gene generates three different mRNAs by alternative splicing of a complex exon. Proc. Natl. Acad. Sci. USA *81*, 5140–5144.

Thumkeo, D., Keel, J., Ishizaki, T., Hirose, M., Nonomura, K., Oshima, H., Oshima, M., Taketo, M., and Narumiya, S. (2003). Targeted disruption of the mouse rho-associated kinase 2 gene results in intrauterine growth retardation and fetal death. Mol. Cell. Biol. *23*, 5043–5055.

Thumkeo, D., Shimizu, Y., Sakamoto, S., Yamada, S., and Narumiya, S. (2005). ROCK-I and ROCK-II cooperatively regulate closure of eyelid and ventral body wall in mouse embryo. Genes Cells *10*, 825–834.

Toomre, D., and Manstein, D. J. (2001). Lighting up the cell surface with evanescent wave microscopy. Trends Cell Biol. *11*, 298–303.

Tsuji, T., *et al*. (2002). ROCK and mDia1 antagonize in Rho-dependent Rac activation in Swiss 3T3 fibroblasts. J. Cell Biol. *157*, 819–830.

Vouret-Craviari, V., Boulter, E., Grall, D., Matthews, C., and Van Obberghen-Schilling, E. (2004). ILK is required for the assembly of matrix-forming adhesions and capillary morphogenesis in endothelial cells. J. Cell Sci. *117*, 4559–4569.

Wierzbicka-Patynowski, I., and Schwarzbauer, J. E. (2002). Regulatory role for src and phosphatidylinositol 3-kinase in initiation of fibronectin matrix assembly. J. Biol. Chem. *277*, 19703–19708.

Wilde, C., and Aktories, K. (2001). The Rho-ADP-ribosylating C3 exoenzyme from *Clostridium botulinum* and related C3-like transferases. Toxicon *39*, 1647–1660.

Yoneda, A., Multhaupt, H.A.B., and Couchman, J. R. (2005). The Rho kinases I and II regulate different aspects of myosin II activity. J. Cell Biol. *170*, 443–453.

Zhang, Q., Magnusson, M. K., and Mosher, D. F. (1997). Lysophosphatidic acid and microtubule-destabilizing agents stimulate fibronectin matrix assembly through Rho-dependent actin stress fiber formation and cell contraction. Mol. Biol. Cell *8*, 1415–1425.

Zhang, Y.-M., *et al*. (2006). Targeted deletion of ROCK1 protects the heart against pressure overload by inhibiting reactive fibrosis. FASEB J. *20*, 916–925.

Zhong, C., Chrzanowska-Wodnicka, M., Brown, J., Shaub, A., Belkin, A. M., and Burridge, K. (1998). Rho-mediated contractility exposes a cryptic site in fibronectin and induces fibronectin matrix assembly. J. Cell Biol. *141*, 539–551.